JOURNAL OF Materials CHEMISTRY

Studies on the structural stability of mesoporous molecular sieves organically functionalized by a direct method

Naoko Igarashi,[a] Kazuhito Hashimoto[a] and Takashi Tatsumi*[b]

[a]*Research Center for Advanced Science and Technology, The University of Tokyo, 4-6-1 Komaba, Meguro-ku, Tokyo, 153-8904, Japan*
[b]*Division of Materials Science & Engineering, Graduate School of Engineering, Yokohama National University, 79-5 Tokiwadai, Hodogaya-ku, Yokohama, 240-8501, Japan. E-mail: ttatsumi@ynu.ac.jp*

Received 5th August 2002, Accepted 10th October 2002
First published as an Advance Article on the web 5th November 2002

The structural stability of mesoporous molecular sieves organically functionalized by a direct method has been investigated in terms of the stability against moisture treatment and mechanical pressure. Incorporation of organic groups directly attached to Si atoms by the use of organosilanes results in an enhancement of the structural stability compared to purely inorganic ones, this enhancement could be ascribed to an increase in hydrophobicity. By pH adjustment and hydrothermal treatment, a further improvement in the stability is attained. A clear relationship between the structural stability and the amount of monolayer adsorption capacity for water is observed. Organically functionalized samples show a lower monolayer adsorption capacity for water than purely inorganic materials, even though both have the same amount of silanol groups, this is probably due to the water-repelling ability of the surface organic groups.

The discovery of a new family of mesoporous molecular sieves such as M41S[1] and FSM-16[2] has received much attention. These materials have high internal surface areas, favorable uniformity and easily controllable pore sizes in the range of 16–100 Å. Because of these peculiar characteristics, the synthesis and application of mesoporous molecular sieves have been investigated by a large numbers of researchers.

In order to make use of these mesoporous molecular sieves as supports, adsorbents, and catalysts, as in the case of conventional microporous zeolites, their structural stability is one of their most significant properties. Although Davis *et al.*[3] reported that pure-silica MCM-41 had a high thermal stability, enough to be heated to at least 850 °C in dry air before the collapse of the structure, MCM-41 has been reported to have a lower mechanical strength[4–6] and a lower hydrothermal stability than zeolites.[3,7,8]

We have already proposed that the structural collapse involves silicate hydrolysis by water adsorbed onto the silanol groups.[9] In addition, we have succeeded in greatly improving the structural stability of MCM-41 materials by post-synthetic trimethylsilylation.[10] On the other hand, various kinds of organically functionalized MCM-41 materials have recently been directly prepared,[11–16] and these are expected to be alternatives to the structurally stabilized trimethylsilylated materials. Therefore, we have investigated the structural stability of these directly organically functionalized MCM-41 materials in terms of their stability against moisture treatment and mechanical pressure in comparison with that of the conventional purely inorganic MCM-41 samples.[17] Here we report the detailed study of the structural stability of organically functionalized MCM-41 materials, mainly focusing on the surface chemistry of the materials investigated by spectroscopic and adsorption techniques.

Experimental

Synthesis

Organically functionalized MCM-41 materials were synthesized by direct methods. The standard synthesis method is as follows: an aqueous solution of NaOH and cetyltrimethylammonium bromide (CTMABr) was added to a mixture of tetraethyl orthosilicate (TEOS) and organosilane, either methyltriethoxysilane (MTES), methyltrimethoxysilane (MTMS) or vinyltriethoxysilane (VTES), under stirring, and this mixture (0.8 TEOS : 0.2 organosilane : 0.12 CTMABr : 0.50 NaOH : 130 H_2O) was aged for 3 days at room temperature. The products were filtered, washed, and dried at 100 °C. The organic templates were removed by acid extraction using 1 M HCl solution in ethanol at 80 °C for about 16 h. The liquid-to-solid ratio was 300 ml g^{-1}. The samples synthesized by this method were named as MCM-41-MTES-AT, where the MTES indicates the organosilane used and the -A and -T at the end of the name mean that the sample was synthesized following procedures of pH adjustment and hydrothermal treatment (at 90 °C for 1 day), respectively. In the pH adjustment,[18] acetic acid was added dropwise to the gel under vigorous stirring until the pH was decreased to 10.2. In the synthesis of MCM-41-40MTES, the percentage of MTES to the total Si source was 40%, twice as much as the usual amount.

Characterization

Samples were characterized by X-ray powder diffraction (XRD), N_2 and H_2O adsorption and ^{13}C and ^{29}Si MAS NMR. XRD patterns were taken on a Rigaku Rint 2400 diffractometer and a Mac Science M3X HF-22E instrument equipped with a Cu Kα X-ray source. Pore sizes, pore volumes, and BET surface areas were estimated from N_2 adsorption isotherms obtained with a Bel Japan BEL SORP 28SA instrument. The pore size distribution from N_2 adsorption was calculated from the corrected Kelvin equation proposed by Kruk *et al.*[19,20] H_2O adsorption measurements were taken with a Bel Japan BEL SORP 18 instrument. ^{13}C CP-MAS and ^{29}Si MAS NMR spectra were recorded on JEOL JNM-L-400WB and JNM-GX270 spectrometers operating at frequencies of 100.53 and 53.54 MHz, respectively. Chemical shifts were referenced to external tetramethylsilane (TMS) for both ^{13}C and ^{29}Si. Spinning rates of 5.2 and 3.5 kHz, recycle delay times of 4.0 and 7.0 s, pulse widths of 5.0 and 6.0 μs, and 1000 and

Table 1 Pore size study for MCM-41 and organically functionalized MCM-41-R samples.[a]

Sample	d_{100}/Å	a_0/Å	S_{BET}/m^2 g^{-1}	V_p/ml g^{-1}	W/Å	Pore wall t/Å	SiOH content (mol %-Si)	R content (mol%-Si)	Peak intensity (100) reflection (%)
MCM-41	37	43	1271	1.12	36	7	67	—	80
MCM-41-A	39	45	932	0.60	34	11	38	—	100
MCM-41-AT	41	47	926	0.74	38	9	42	—	94
MCM-41-MTES	34	40	1192	0.76	31	9	53	12.5	65
MCM-41-VTES	33	38	1225	0.70	29	9	50	7.1	78
MCM-41-MTES-A	35	41	1169	0.85	31	10	41	14.8	65
MCM-41-MTES-T	36	41	942	0.51	30	12	59	11.8	73
MCM-41-MTES-AT	36	42	1251	0.72	32	10	45	16.1	99
MCM-41-40MTES	33	38	1266	0.64	27	11	32	34.8	29
MCM-41-MTMS	35	41	1266	0.73	35	6	49	9.4	82
MCM-41-MTMS-AT	37	43	1114	0.68	34	9	43	13.1	85

[a] a_0/Å, unit cell length = $d_{100} \times 2/\sqrt{3}$; V_p, primary mesopore volume obtained from t-plot method; W, pore diameter determined from BJH method (N_2 adsorption); pore wall thickness t/Å = $a_0 - W$; SiOH content (mol%-Si) = $(2Q^2 + Q^3)/(Q^2 + Q^3 + Q^4) \times 100\%$; R content (mol%-Si) = T/(T + Q) × 100%.

15000–20000 scans were taken for ^{13}C and ^{29}Si, respectively. The ^1H contact time in the ^{13}C CP-MAS NMR measurements was 3 ms.

The stability against moisture was evaluated by exposing the samples to moisture over a saturated aqueous solution of NH_4Cl at room temperature for various times in days, followed by various methods of chracterization to observe the changes. The mechanical stability was investigated by compressing the samples under various pressures under an atmosphere of air; 0.1 g of the samples were pressed in a steel die of 20 mm diameter for 10 min.

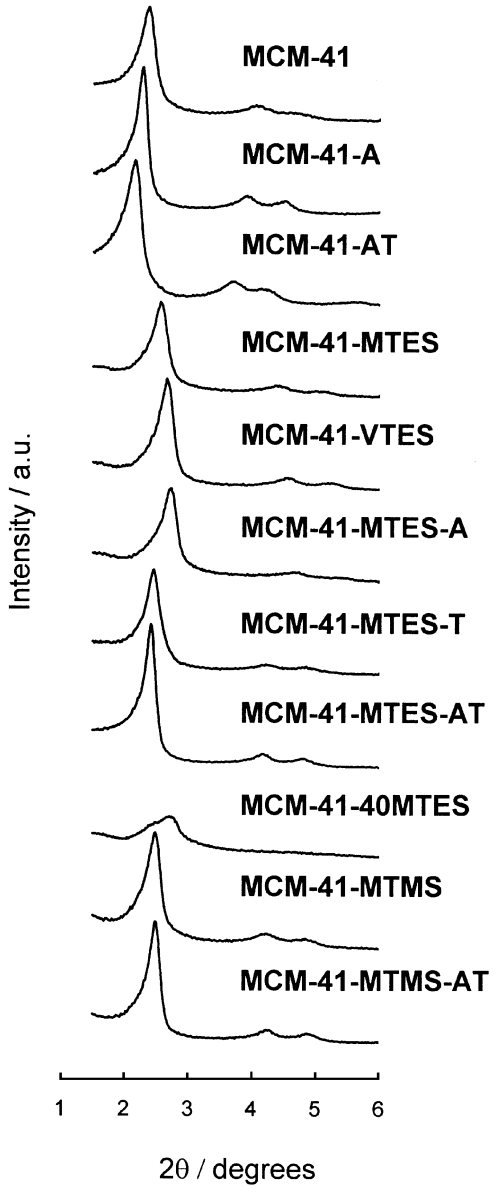

Fig. 1 Powder X-ray diffraction patterns of the MCM-41 materials.

Results and discussion

Physical properties

The physical properties of the organically functionalized MCM-41 samples are summarized in Table 1. The organically modified samples exhibit low peak intensities for the (100) reflections compared to the purely inorganic ones (Fig. 1). This low order of regularity would be due to the limitation of siloxane bond formation, *i.e.*, one SiOH group inevitably accompanies one Si–R bonding. Thus, the addition of organosilane eventually results in structural irregularity. The incorporation of the methyl group results in unit cell contraction; the increased chain length from the methyl group to the vinyl group gives rise to additional contraction. The organically functionalized materials have a smaller pore size and pore volume than the purely inorganic ones. Recently, Richer and Mercier[21] suggested that the interaction between the organic groups and the hydrophobic alkyl groups of the micelles resulted in contraction of the pore diameter of organically modified mesoporous materials. As shown in Scheme 1, the presence of organic groups is likely to result in a deeper penetration of the organosiloxane-derived molecules into the micelle than that of TEOS-derived molecules due to a repulsive interaction at the interface of the inorganic–organic double layer.

The acetic acid treatment gives materials with larger (100) d-spacing (d_{100}) as reported by Ryoo and Kim.[18] In addition, pore wall thickening is observed; for MCM-41-A the difference

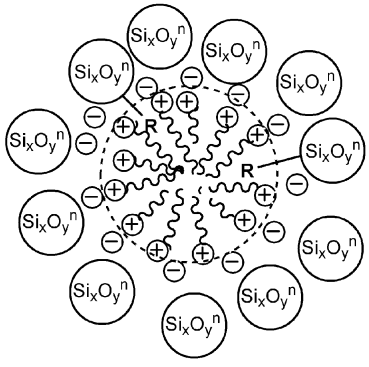

Scheme 1 Diagram of the interaction between the organically functionalized silicates and the surfactant molecules.

is 4 Å. The increase in the unit cell also occurs in the hydrothermal treatments for both pure silica and organically modified samples, whereas the pore sizes (W) of the organically functionalized samples are not increased (*i.e.*, W = 31, 30, 32 Å for MCM-41-MTES, MCM-41-MTES-T and MCM-41-MTES-AT, and W = 35 and 34 Å for MCM-41-MTMS and MCM-41-MTMS-AT, respectively), indicating that pore wall thickening occurs. The pore size retention for the organically functionalized samples with/without hydrothermal treatment, which was not observed in pure silica materials, is probably due to pore size contraction in the presence of organosilanes,[21] compensated by pore size enlargement due to the size growth of the micelle at higher temperatures, based on the Debye–Hückel theory.

The direct incorporation of organic groups is confirmed by the ^{13}C and ^{29}Si MAS NMR. ^{29}Si MAS NMR spectra of the organically functionalized samples show five peaks which can be assigned to $Si(OSi)_4$ [Q^4], $HOSi(OSi)_3$ [Q^3], $(HO)_2Si(OSi)_2$ [Q^2], $RSi(OSi)_3$ [T^3], and $R(HO)Si(OSi)_2$ [T^2], respectively (Fig. 2). The degree of organosiloxane incorporation was determined from the percentage of T-type peak area to the total peak area due to T^m and Q^n species. The pH adjustment by acetic acid slightly increased the degree of organic group incorporation without decreasing the structural regularity (14.8 mol%-$MeSiO_3$ for MCM-41-MTES-A) in comparison with the standard synthesis (12.5 mol%-$MeSiO_3$ for MCM-41-MTES). The rate of hydrolysis of organoalkoxysilanes under basic conditions is slower than that of tetraalkoxysilanes due to the higher basicity at the silicon center because of the presence of organic groups directly bonded to Si.[22] This would lead to the formation of MCM-41 materials with lower organic contents than their starting gels. pH adjustment beneficially affects the condensation of silicates and the product yield[18] by shifting the silicate condensation reaction equilibrium which is highly sensitive to pH, seemingly without discriminating between organosilanes and inorganic ones. The product yield increases from 63% to 85% on acetic acid treatment (MCM-41-MTES and MCM-41-MTES-A). It is considered that this increase in the product yield gives rise to the slightly increased degree of organic group incorporation by pH adjustment.

The hydrolysis and condensation rates for organosilanes are usually slower than those of TEOS under basic conditions. However, the differences in the rates between organosilanes and TEOS should become smaller with increasing temperature. Therefore, it was considered that the organic content could be increased by conducting the synthesis at a higher temperature; on the other hand, the hydrothermal process results in a slight decrease in the amount of organic group incorporation (11.8 mol%-$MeSiO_3$ for MCM-41-MTES-T). However, hydrothermal treatment enhances the degree of organic functionalization when combined with acetic acid treatment (16.1 mol%-$MeSiO_3$ for MCM-41-MTES-AT). The increased intensities of the (100) reflection are observed for either of the hydrothermally treated or the pH adjusted samples, and the highest peak intensity for the sample applied both treatments (Table 1).

MTMS is used to increase the organic group incorporation since the methoxy group in MTMS is expected to be more reactive to hydrolysis than the ethoxy group in MTES; however, the use of MTMS resulted in a decreased incorporation of the methyl group (9.4 mol%-$MeSiO_3$ for MCM-41-MTMS, 12.5 mol%-$MeSiO_3$ for MCM-41-MTES).

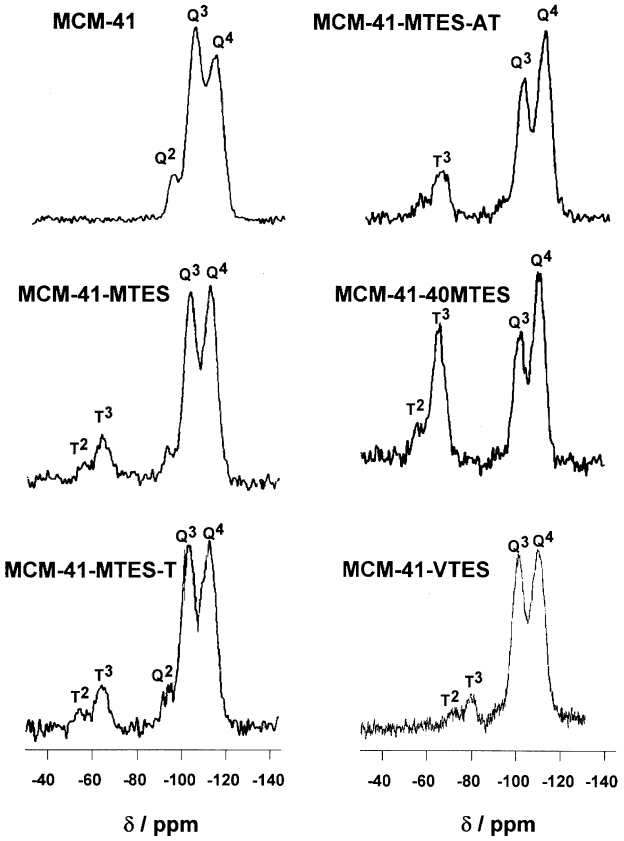

Fig. 2 ^{29}Si MAS NMR spectra of various MCM-41-R samples.

Stability against moisture

Fig. 3 shows the change in the peak intensity of the (100) reflection during water vapor treatment of purely inorganic and organically functionalized MCM-41 materials. Direct incorporation of organic groups into the MCM-41 materials leads to an improvement in stability (MCM-41-MTES, MCM-41-VTES, MCM-41-MTMS). There is no distinct difference in the stability towards water observed between the samples containing vinyl or methyl groups although the vinyl group incorporation is half as much as the methyl group incorporation (7.1 and 12.5 mol%, respectively). When the organosilane : TEOS ratio is increased to 40 : 60, organic group incorporation is dramatically enhanced, although the XRD pattern shows a decreased structural regularity (Fig. 1).

Both pH adjustment and hydrothermal treatment greatly

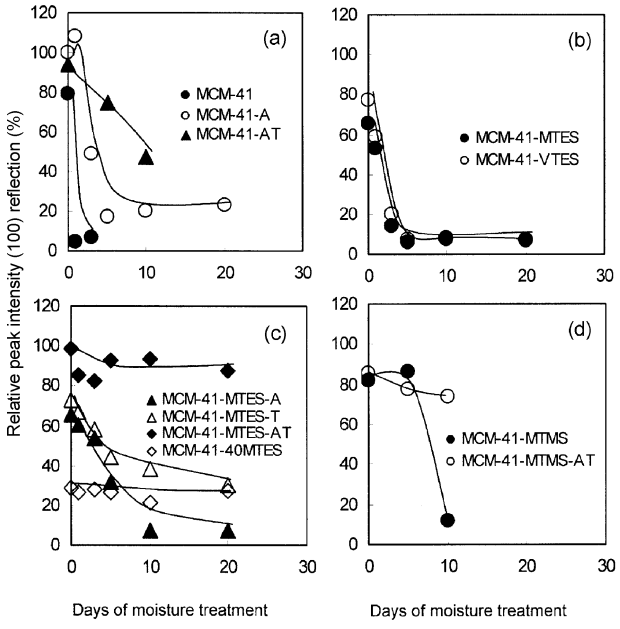

Fig. 3 Change in peak intensity of the (100) reflections of moisture treated samples. (a) A series of pure silica MCM-41, (b) and (c) a series of organically functionalized MCM-41-R samples synthesized from MTES and VTES, and (d) MTMS.

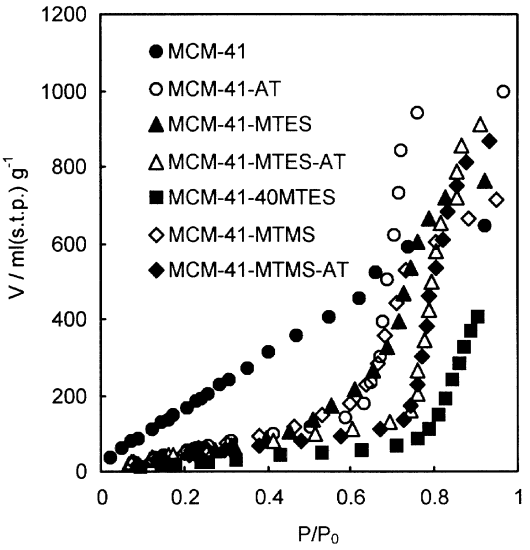

Fig. 4 H_2O adsorption isotherms of MCM-41 and organically functionalized MCM-41-R samples.

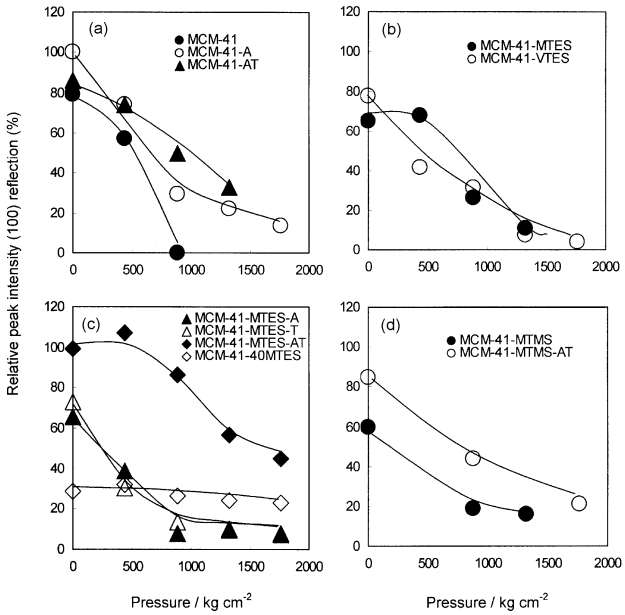

Fig. 5 Change in peak intensity of the (100) reflections of mechanically compressed samples. (a) A series of pure silica MCM-41, (b) and (c) a series of organically functionalized MCM-41-R samples synthesized from MTES and VTES, and (d) MTMS.

enhances the stability to moisture of the organic-group-containing MCM-41 materials. In particular, the combination of both treatments effectively yields the highly stable material MCM-41-MTES-AT, as shown in Fig. 3c. The high stability is attributed to an enhancement of the condensation of silicates and also to the resultant organic group incorporation increase, as shown in Table 1.

The H_2O adsorption isotherms (Fig. 4) clearly show that purely inorganic MCM-41 has a higher affinity towards water than other materials, such as MCM-41-40MTES, MCM-41-MTES-AT and MCM-41-MTMS-AT, which demonstrate highly hydrophobic characteristics in the H_2O adsorption isotherms with very little adsorption of water in the relative pressure range P/P_0 of 0–0.6; these results are in good agreement with their high structural stability to moisture.

The physical properties of the materials after moisture treatment are summarized in Table 2. As shown in Table 2, after moisture treatment, a dramatic decrease is observed not only in d_{100} and W but also in BET surface area (S_{BET}) and pore volume (V_p), except for structurally stable MCM-41-MTES-AT and MCM-41-40MTES, suggesting a severe structural collapse. For the pure silica MCM-41, a structural deterioration (70% loss of S_{BET} and 82% loss of V_p) was observed after 3 days of moisutre treatment (Table 2). Organic functionalization mitigates the decrease in the BET surface area (1–59% loss) and pore volume (8–66% loss of V_p). MCM-41-VTES also demonstrates a remarkable retention of S_{BET} and V_p (1 and 29% loss, respectively) after treatment; however, a severe contraction of the unit cell and pore size was observed. Among the organically functionalized samples, MCM-41-MTES-AT and MCM-41-40MTES showed the least structural loss, as judged from N_2 adsorption measurements, being in good agreement with the results based on the d_{100} reflection intensity in the powder XRD patterns.

Stability against mechanical pressure

Fig. 5 shows the changes in d_{100} peak intensity of the mechanically compressed pure silica MCM-41 and organic group-containing MCM-41 samples. The organic modification of the original synthesis method by adding MTES, MTMS or VTES improved the mechanical stability. A combination of acetic acid treatment and hydrothermal treatment gives the material with the highest mechanical stability (MCM-41-MTES-AT), whereas the merely hydrothermally treated sample (MCM-41-MTES-T) or acetic acid treated sample MCM-41-MTES-A collapse relatively easily by compression. The sample with increased organosilane : TEOS ratio also showed high mechanical stability.

Koyano *et al.*[9] reported that MCM-41 and MCM-48 collapsed mechanochemically due to water adsorbed onto the silanol groups for a mechanically pressed material. As shown in Fig. 6, the *d*-spacing remained virtually unchanged through compression at various pressures, suggesting some parts of the material remained intact while other parts were totally crushed, giving rise to nonporous structures. Desplantier-Giscard *et al.*[5] reported a similar observation. In contrast, a large decrease in *d*-spacing and pore size of the materials was

Table 2 Pore size study for moisture treated MCM-41 and organically functionalized MCM-41-R samples.[a]

Sample [days of moisture treatment]	d_{100}/Å	a_0/Å	S_{BET}		V_p		W/Å
			$m^2\ g^{-1}$	loss (%)	ml g^{-1}	loss (%)	
MCM-41 [3]	n.d.[b]		386	70	0.20	82	22
MCM-41-MTES [20]	29	34	724	39	0.34	55	23
MCM-41-VTES [20]	27	32	1212	1	0.50	29	24
MCM-41-MTES-A [20]	n.d.[b]		475	59	0.29	66	20
MCM-41-MTES-T [20]	32	37	660	30	0.39	24	27
MCM-41-MTES-AT [20]	37	43	915	27	0.53	26	31
MCM-41-40MTES [20]	32	37	1159	8	0.59	8	27

[a] a_0/Å, unit cell length = $d_{100} \times 2/\sqrt{3}$; V_p, primary mesopore volume obtained from *t*-plot method; W, pore diameter determined from BJH method (N_2 adsorption); loss, the amount of loss in % of S_{BET} and V_p during moisture treatment. [b]Not determined.

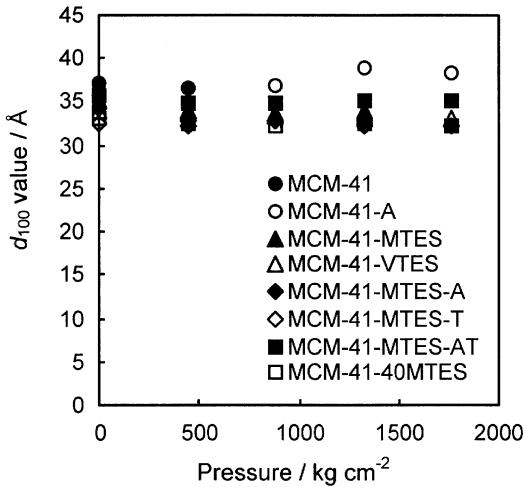

Fig. 6 Change in d_{100} value of the mechanically compressed MCM-41materials.

observed for moisture treatment (Table 2). Even though the stability to mechanical compression and moisture treatment has revealed a similar tendency, presumably different mechanisms operate in the structural collapse between mechanical compression and moisture treatment.

Surface coverage of silanol and organic groups

In Fig. 7, the amount obtained from the addition of a number of silanol groups (per nm^2), [SiOH], and the organic groups attached to Si atoms (per nm^2), [R], are shown for selected samples according to the same synthetic parameters (*i.e.*, synthesis temperature and pH adjustment). [SiOH] and [R] (per nm^2) were estimated by the following formulae:

$$\mathrm{SiOH(molecules/nm^2)} = \frac{6.023\times10^5\times(I_{Q3}+I_{Q2}\times2+I_{T2})}{(60\times I_{Q4}+69\times I_{Q3}+78\times I_{Q2}+67\times I_{T3}+76\times I_{T2})\times \mathrm{BET\ SA}};$$

$$\mathrm{R\ (molecules/nm^2)} = \frac{6.023\times10^5\times(I_{T3}+I_{T2})}{(60\times I_{Q4}+69\times I_{Q3}+78\times I_{Q2}+67\times I_{T3}+76\times I_{T2})\times \mathrm{BET\ SA}}$$

where I_i represents the relative peak area of the corresponding silicon species in the ^{29}Si MAS NMR spectra. It can be clearly seen that the sum of [SiOH] and [R] is roughly constant (5–4.5) for samples synthesized under same conditions (*ca.* 5 for samples synthesized at room temperature: MCM-41, MCM-41-MTES, and MCM-41-40MTES and *ca.* 4.5 for acid- and hydrothermally-treated samples: MCM-41-AT, MCM-41-MTES-AT, and MCM-41-MTMS-AT, respectively). These

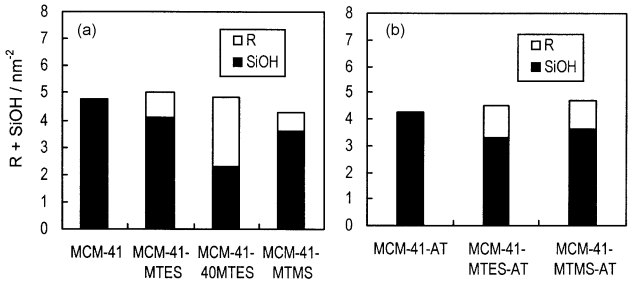

Fig. 7 The amount obtained from the addition of SiOH (nm^2) and R groups of samples: (a) synthesized at room temperature; and (b) acetic acid and hydrothermally treated.

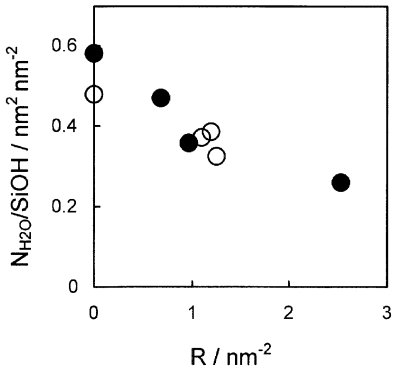

Fig. 8 Comparison of the relation between the ratio of N_{H_2O} : OH (based on water adsorption and ^{29}Si-MAS NMR) and the amount of R group (nm^2) (obtained by ^{29}Si-MAS NMR) for samples synthesized at room temperature (●) and samples treated pH adjustment and hydrothermal (○).

results strongly indicate that [R] successfully replaced a part of [SiOH] without creating additional silanol groups.

The monolayer adsorption capacity for water (molecule nm^{-2}), [N_{H_2O}], is estimated by the H_2O adsorption and BET surface area (m^2 g^{-1}). In Fig. 8, the [N_{H_2O}] : [SiOH] ratio is plotted against [R]. The [N_{H_2O}] : [SiOH] ratio decreases linearly with increasing amounts of [R]. This is probably due to the water repelling ability of organic groups; the R group could shield the silanol groups present on the surface from H_2O (Scheme 2). This water-repelling effect together with the substitution of R for a hydroxy group leads to the stabilization of the structural regularity.

The [N_{H_2O}] : [SiOH] ratio is 0.5–0.6 for the pure silica materials (Fig. 8), suggesting a relationship close to a 1 : 2 ratio between the water molecules and the surface silanol groups, which is also observed in the densely hydroxylated silica surface.[23–28] Such a ratio, less than 1, is probably due to the large amount of hydrogen-bonded silanol groups present on our samples.

Fig. 9 shows the IR spectrum of a pure silica MCM-41 sample measured after outgassing at 200 °C. The large broad peaks in the range of 3600–3700 cm^{-1} are attributable to hydrogen-bonded silanol groups.

The density of SiOH (nm^2) over purely inorganic MCM-41 and organically functionalized MCM-41-RTES based on ^{29}Si MAS NMR is 4.2–4.8 and 2.8–4.1, respectively. The former is slightly less than that on a silica surface (between 5 and 8 nm^2) and higher than the density reported by Zhao *et al.*[29,30] (2.5 and 3.0 nm^2) and Ishikawa *et al.*[6] (3.3 nm^2). The significantly higher [SiOH] observed in this study may be due to the low temperature conditions for removing the templates (80 °C in ethanol–HCl solution) and for drying (100 °C). However, due to the water-repelling effect of the R group, the amount of unshielded silanol groups, which can interact with H_2O, is much smaller than the amount of SiOH groups observed by ^{29}Si NMR and inversely related to the amount of R-group.

Apparently water adsorbed onto the silanol groups causes the hydrolysis of nearby Si–O–Si bonds, resulting in the

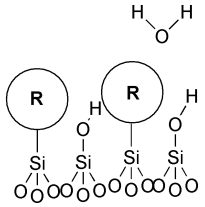

Scheme 2 Suggested structure for the SiOH groups and water molecules in the presence of the R group.

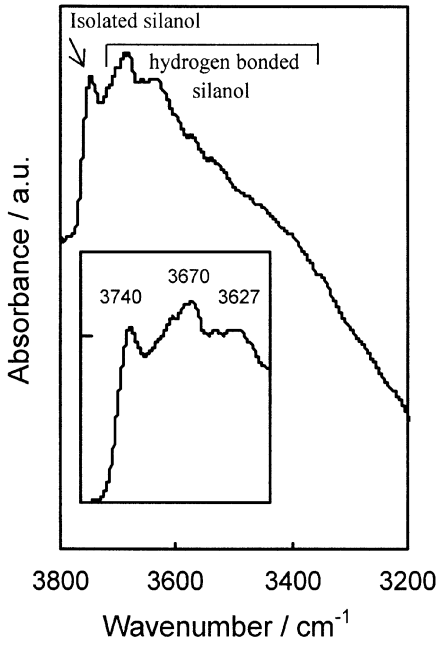

Fig. 9 IR spectrum of pure silica MCM-41 measured after evacuation at 200 °C.

collapse of the ordered mesoporous structure.[10] A high structural irregularity is associated with increased silanol groups, which gives rise to increased water adsorption onto the silanol groups. This will be a key factor in eventually causing the hydrolysis of the Si–O–Si bonds in the MCM-41 framework. In contrast, a structurally ordered surface, where less silanol groups are present, may be more resistant to destruction than a less ordered surface. Alternatively, organic groups such as methyl or vinyl possibly shield the material surface as shown above, thereby protecting the Si–O–Si bonds from attack by nearby water molecules. Therefore, a more ordered structure, or materials containing more organic groups, would be more resistant to moisture and mechanical pressure.

Conclusion

Mesoporous molecular sieve MCM-41 was organically functionalized by a direct method, and its structural stability was investigated in terms of the stability against moisture treatment and mechanical pressure. Organically functionalized samples showed an enhanced structural stability and a lower monolayer adsorption capacity for water compared with purely inorganic materials, probably due to the water-repelling ability of the surface organic groups. A clear relationship between the structural stability and the monolayer adsorption capacity for water was observed. A further improvement in the stability was attained by pH adjustment and hydrothermal treatment. Thus the synthesized highly stable MCM-41 materials would be practically applicable for use as adsorbents under hydrothermal conditions, catalysts for liquid phase reactions, and also low-k materials.

References

1 J. S. Beck, J. C. Vartuli, W. J. Roth, M. E. Leonowicz, C. T. Kresge, K. D. Schmitt, C. T.-U. Chu, D. H. Olson, E. W. Sheppard, S. B. McCullen, J. B. Higgins and J. L. Schlenker, *J. Am. Chem. Soc.*, 1992, **114**, 10834.
2 S. Inagaki, Y. Fukushima and K. Kuroda, *Chem. Commun.*, 1993, 680.
3 C. Y. Chen, H. X. Li and M. E. Davis, *Microporous Mater.*, 1993, **2**, 17.
4 V. Y. Gusev, X. Feng, Z. Bu, G. L. Haller and J. A. O'Brien, *J. Phys. Chem.*, 1996, **100**, 1985.
5 D. Desplantier-Giscard, O. Collart, A. Galarneau, P. Van Der Voort, F. Di Renzo and F. Fajula, *Stud. Surf. Sci. Catal.*, 2000, **129**, 665.
6 T. Ishikawa, M. Matsuda, A. Yasukawa, K. Kandori, S. Inagaki, T. Fukushima and S. Kondo, *J. Chem. Soc., Faraday Trans.*, 1996, **92**, 1985.
7 J. M. Kim, J. H. Kwak, S. Jun and R. Ryoo, *J. Phys. Chem.*, 1995, **99**, 16742.
8 J. M. Kim and R. Ryoo, *Bull. Korean Chem. Soc.*, 1996, **17**, 66.
9 T. Tatsumi, K. A. Koyano, Y. Tanaka and S. Nakata, *Chem. Lett.*, 1997, 469.
10 K. A. Koyano, T. Tatsumi, Y. Tanaka and S. Nakata, *J. Phys. Chem., B.*, 1997, **101**, 9436.
11 S. L. Burkett, S. D. Sims and S. Mann, *Chem. Commun.*, 1996, 1367.
12 D. J. Macquarrie, *Chem. Commun.*, 1996, 1961.
13 M. H. Lim, C. F. Blanford and A. Stein, *J. Am. Chem. Soc.*, 1997, **119**, 4090.
14 S. Inagaki, S. Guan, Y. Fukushima, T. Ohsuna and O. Terasaki, *J. Am. Chem. Soc.*, 1999, **121**, 9611.
15 B. J. Melde, B. T. Holland, C. F. Blanford and A. Stein, *Chem. Mater.*, 1999, **11**, 3302.
16 T. Asefa, M. J. MacLachlan, N. Coombs and G. A. Ozin, *Nature*, 1999, **402**, 867.
17 N. Igarashi, Y. Tanaka, S. Nakata and T. Tatsumi, *Chem. Lett.*, 1999, 1.
18 R. Ryoo and J. M. Kim, *Chem. Commun.*, 1995, 711.
19 M. Kruk, M. Jaroniec and A. Sayari, *Langmuir*, 1997, **13**, 6267.
20 M. Kruk, M. Jaroniec and A. Sayari, *J. Phys. Chem., B*, 1997, **101**, 583.
21 R. Richer and L. Mercier, *Chem. Commun.*, 1998, 1775.
22 C. J. Brinker and G. W. Scherer, in *Sol-Gel Science: The Physics and Chemistry of Sol-Gel Processing*, Academic Press, Boston, 1990, p.123.
23 K. Klier, H. J. Shen and A. C. Zettlemoyer, *J. Phys. Chem.*, 1973, **77**, 1458.
24 D. R. Bassett, E. A. Boucher and A. C. Zettlemoyer, *J. Colloid Interface Sci.*, 1970, **34**, 436.
25 D. R. Bassett, E. A. Bocher and A. C. Zettlemoyer, *J. Colloid Interface Sci.*, 1968, **27**, 649.
26 A. C. Zettlemoyer, *J. Colloid Interface Sci.*, 1968, **28**, 4.
27 A. V. Kiselev and V. I. Lygin, *Kolloidn. Zh.*, 1959, **21**, 561.
28 H. Naono, R. Fujiwara and M. J. Yagi, *J. Colloid Interface Sci.*, 1980, **76**, 74.
29 X. S. Zhao, G. Q. Lu, A. K. Whittaker, G. J. Millar and H. Y. Zhu, *J. Phys. Chem., B*, 1997, **101**, 6525.
30 X. S. Zhao and G. Q. Lu, *J. Phys. Chem., B*, 1998, **102**, 1556.